Journal of Controlled Release 323 (2020) 624–634

Contents lists available at ScienceDirect

Journal of Controlled Release

journal homepage: www.elsevier.com/locate/jconrel

Preclinical antitumor efficacy of senescence-inducing chemotherapy combined with a nanoSenolytic

Irene Galiana[a,b], Beatriz Lozano-Torres[a,b,c], Mónica Sancho[b,d], María Alfonso[a], Andrea Bernardos[a,b], Viviana Bisbal[d], Manuel Serrano[f], Ramón Martínez-Máñez[a,b,c,e,*], Mar Orzáez[b,d,*]

[a] Instituto Interuniversitario de Investigación de Reconocimiento Molecular y Desarrollo Tecnológico (IDM), Universitat Politècnica de València, Universitat de València, Camino de Vera s/n, 46022, Valencia, Spain
[b] Unidad Mixta UPV-CIPF de Investigación en Mecanismos de Enfermedades y Nanomedicina, Universitat Politècnica de València, Centro de Investigación Príncipe Felipe, C/ Eduardo Primo Yúfera 3, 46012, Valencia, Spain
[c] CIBER de Bioingeniería, Biomateriales y Nanomedicina (CIBER-BBN), Spain
[d] Centro de Investigación Príncipe Felipe, C/ Eduardo Primo Yúfera 3, 46012, Valencia, Spain
[e] Unidad Mixta de Investigación en Nanomedicina y Sensores, Universitat Politècnica de València, IIS La Fe. Av. Fernando Abril Martorell, 106 Torre A 7ª planta, 46026, Valencia, Spain
[f] Institute for Research in Biomedicine (IRB Barcelona), Barcelona Institute of Science and Technology (BIST), Catalan Institution for Research and Advanced Studies (ICREA), Barcelona, Spain

ARTICLE INFO

Keywords:
Breast Cancer
Mesoporous silica nanoparticles
Senescence
Senolysis

ABSTRACT

The induction of senescence produces a stable cell cycle arrest in cancer cells, thereby inhibiting tumor growth; however, the incomplete immune cell-mediated clearance of senescent cells may favor tumor relapse, limiting the long-term anti-tumorigenic effect of such drugs. A combination of senescence induction and the elimination of senescent cells may, therefore, represent an efficient means to inhibit tumor relapse. In this study, we explored the antitumor efficacy of a combinatory senogenic and targeted senolytic therapy in an immunocompetent orthotopic mouse model of the aggressive triple negative breast cancer subtype. Following palbociclib-induced senogenesis and senolysis by treatment with nano-encapsulated senolytic agent navitoclax, we observed inhibited tumor growth, reduced metastases, and a reduction in the systemic toxicity of navitoclax. We believe that this combination treatment approach may have relevance to other senescence-inducing chemotherapeutic drugs and additional tumor types.

Significance: While the application of senescence inducers represents a successful treatment strategy in breast cancer patients, some patients still relapse, perhaps due to the subsequent accumulation of senescent cells in the body that can promote tumor recurrence. We now demonstrate that a combination treatment of a senescence inducer and a senolytic nanoparticle selectively eliminates senescent cells, delays tumor growth, and reduces metastases in a mouse model of aggressive breast cancer. Collectively, our results support targeted senolysis as a new therapeutic opportunity to improve outcomes in breast cancer patients.

1. Introduction

Cellular senescence is the stable cell cycle arrest that occurs in response to stressful stimuli [1,2]. Many studies have explored induced senescence as a desirable outcome in tumor treatment and several senescence-inducing or senescence-reinforcing drugs have been developed, including telomerase activity inhibitors, tumor suppressor gene re-activators, or cyclin-dependent kinase (CDKs) inhibitors [3,4,73]. The Food and Drug Administration (FDA) recently approved the CDK4/6 inhibitors abemaciclib [5], palbociclib [6], and ribociclib [7] for the treatment of estrogen receptor (ER)-positive metastatic breast cancer in combination with anti-hormonal therapy. Encouragingly, this approach has provided the best progression-free survival (PFS) results to date [8–10]. Specifically, palbociclib is an orally-administered highly-specific inhibitor that blocks CDK4- and CDK6- Cyclin D kinase activity at very low concentrations [6,11]. Due to encouraging pre-clinical results

* Corresponding authors at: Unidad Mixta UPV-CIPF de Investigación en Mecanismos de Enfermedades y Nanomedicina, Universitat Politècnica de València, Centro de Investigación Príncipe Felipe, C/ Eduardo Primo Yúfera 3, 46012, Valencia, Spain.
E-mail addresses: rmaez@qim.upv.es (R. Martínez-Máñez), morzaez@cipf.es (M. Orzáez).

https://doi.org/10.1016/j.jconrel.2020.04.045
Received 2 December 2019; Received in revised form 7 April 2020; Accepted 27 April 2020
Available online 04 May 2020
0168-3659/

[6] and several successful clinical trials [9,12–17], palbociclib is now prescribed as a combination therapy with either letrozole or fulvestrant for the treatment of ER-positive/Her2-negative breast cancer and is in clinical trials for the treatment of triple negative breast cancer (TNBC) patients overexpressing the androgen receptor (AR). TNBC represents one of the most aggressive breast cancer subtypes with a poorer prognosis compared to other breast cancer subtypes and currently lacks effective treatment options.

Despite the proven clinical potential of senescence inducers, senescent cells can play both beneficial and detrimental roles in age-related diseases or cancer [18], a phenomenon known as antagonistic pleiotropy [19]. Following damage to cells during cancer progression or aging, cells initiate a sequence of processes involving the immune system that culminates in senescent cell clearance and tissue regeneration. However, this beneficial process can be corrupted, particularly in aged tissues with a potentially impaired immune system. The unwanted accumulation of senescent cells can prompt tissue dysfunction, reduce effective tissue regeneration, and contribute to the pathogenesis of several diseases [20–24]. The role of the secretory associated senescence phenotype (SASP) also reflects the antagonistic pleiotropic character of senescence. The SASP participates in the clearance of premalignant cells, the reinforcement of the senescence state, and tissue remodeling and repair. However, the SASP can also contribute to tumor progression by stimulating phenotypes associated with aggressive cancer cells, providing an ideal niche for cancer cell proliferation, or promoting the epithelial-to-mesenchymal transition [1,21,23]. Therefore, senescence can be viewed as a double-edged sword, either suppressing or promoting tumor development [24–27]. As the accumulation of senescent cells can prompt an increased risk of carcinogenesis and metastasis [28–30], the long-term improvement of chemotherapeutic and senescence-inducing treatments for cancer treatment will involve the elimination of senescent cells [31].

There are two main therapeutic approaches to attenuate the adverse effects of senescence: senolytic induction, which provokes the direct elimination of senescent cells, and SASP neutralization [24,32]. While senolysis represents a selective and universal method for the elimination of senescent cells and a potentially useful therapy, we currently suffer from a lack of approved senolytic drugs. Among several small molecules displaying senolytic effects *in vitro* and *in vivo* [33], navitoclax potently and specifically inhibits the Bcl-2, Bcl-w, and Bcl-xL anti-apoptotic proteins to promote senolysis [34]. Senescent cell survival depends in many cases on elevated levels of the Bcl-2 family of anti-apoptotic factors, making them hypersensitive to apoptosis induced by Bcl-2 inhibitors [34–37]. While the Bcl-2 family inhibitor navitoclax represents a highly potent senolytic drug, the associated toxic side-effects have prevented FDA approval. In particular, thrombocytopenia represents the significant dose-limiting toxicity derived from the inhibition of Bcl-xL [38,39,74].

The design of nanomaterials as drug carriers with improved pharmacokinetics, bioavailability, and biodistribution has revolutionized the field of controlled drug delivery systems in recent years. Mesoporous silica nanoparticles (MSNs) have proven excellent scaffolds for the development of multifunctional nanodevices for advanced medical applications thanks to advantageous characteristics such as their homogeneous porosity, inert nature, high loading capacity, and facile surface functionalization. Moreover, MSNs can be gated/capped using various molecular strategies that mediate specific cargo release only in the presence of specific physical, chemical, or biochemical stimuli [40–42]. MSNs have been primarily applied in cancer treatment as they passively accumulate in tumors due to the enhanced permeability and retention (EPR) effect. Importantly, enhanced tumor accumulation combined with the site-specific release of cargo reduces any side effects associated with the cargo in healthy tissues [43–45].

In previous collaborative studies from our group, capped MSNs have been tested in several senescence-related disease models such as dyskeratosis congenita [46,47], chemotherapy-treated xenograft tumors, and lung fibrosis [48]. Now, we report a combination therapy comprising a senogenic agent with a nanotherapy-targeted senolytic agent in an immunocompetent orthotopic mouse TNBC model. Senogenesis (senescence induction) induced with the CDK4/6 inhibitor palbociclib and senolysis (selective cell death of senescent cells) with navitoclax encapsulated in MSNs capped with a galactooligosaccharide, allowing selective release in senescent cells. Similar nanoparticles loaded with the indocyanine green (ICG) dye permitted to trace senescent cells *in vivo*. Here, we establish that TNBC treatment with palbociclib followed by the elimination of senescent cells with encapsulated navitoclax inhibits tumor development and reduces metastasis while also diminishing the systemic toxicity of navitoclax.

2. Results

2.1. Palbociclib induces senescence in triple negative breast Cancer cells

The 4 T1 murine breast cancer cell line exhibits a highly aggressive triple-negative profile, and the 4 T1 *in vivo* orthotopic tumor model recapitulates many aspects of the human TNBC [49–52]. The relevance of immunity in the antitumoral response, and particularly upon senescence induction, makes performing studies of tumor evolution in the presence of an intact immune system a fundamental task [53,54]. For this reason, we employed this immunocompetent orthotopic TNBC mouse model for our *in vivo* studies of senoinduction and senolysis.

As only some subtypes of TNBC tumors respond to treatment with CDK4/6 inhibitors [55], we first determined the sensitivity of 4 T1 cells to treatment with palbociclib. Treatment with 5 μM palbociclib prompted the appearance of canonical senescence markers in 4 T1 cells, including the overexpression of the lysosomal β-galactosidase enzyme (SA-βGal) [56,57] (Fig. 1A), an increase in cell size, and a high number of intracellular vesicles [1,20,32]. We also detected reduced levels of proliferation, as evidenced by lower levels of Ki67 immunostaining (Fig. 1B) and accumulation of G1-phase cells by propidium iodide analysis (Fig. 1C), indicative of cell cycle arrest after palbociclib treatment together with a progressive decrease in the levels of phosphorylated retinoblastoma protein (pRb) (Fig. 1D). Clonogenic assays were also performed to confirm cycle arrest in 4 T1 palbociclib-treated cells; to this end, the same number of control and senescent cells were seeded in culture plates and, after one week, we estimated changes to cell number by crystal violet staining. 4 T1 cell cultures treated with palbociclib exhibited lower levels of staining indicative of decreased cellular proliferation and cell cycle arrest (Fig. 1D).

In summary, these results confirm that the treatment of the 4 T1 TNBC cell line with the CDK4/6 inhibitor palbociclib efficiently induces senescence.

2.2. Senolytic treatment of senescent triple negative breast Cancer cells induces cell death

Senescent cells depend on the expression of various pro-survival factors, with the anti-apoptotic activity of the protein Bcl-xL reported in various cell lines [37]. Therefore, we evaluated the protein expression of this anti-apoptotic Bcl-2 family protein member in palbociclib-treated 4 T1 cells *via* Western blotting. As expected, we observed a significant increase in Bcl-xL protein expression following the induction of senescence by palbociclib exposure (Fig. 2A); however, an accompanying increase in the expression of the pro-apoptotic BH3-only protein Bim was also detected. The obtained Bcl-2 protein profile is consistent with a phenotype attributed to “primed cells” that exhibit a dependence on anti-apoptotic proteins for survival and display high sensitivity to BH3 mimetic drugs such as navitoclax [58,59].

We next explored the inhibition of Bcl-2 anti-apoptotic proteins by free navitoclax (Nav) as a strategy to selectively induce cell death in senescent 4 T1 cells. We first analyzed mitochondrial functionality following exposure of 4 T1 cells to free navitoclax by flow cell

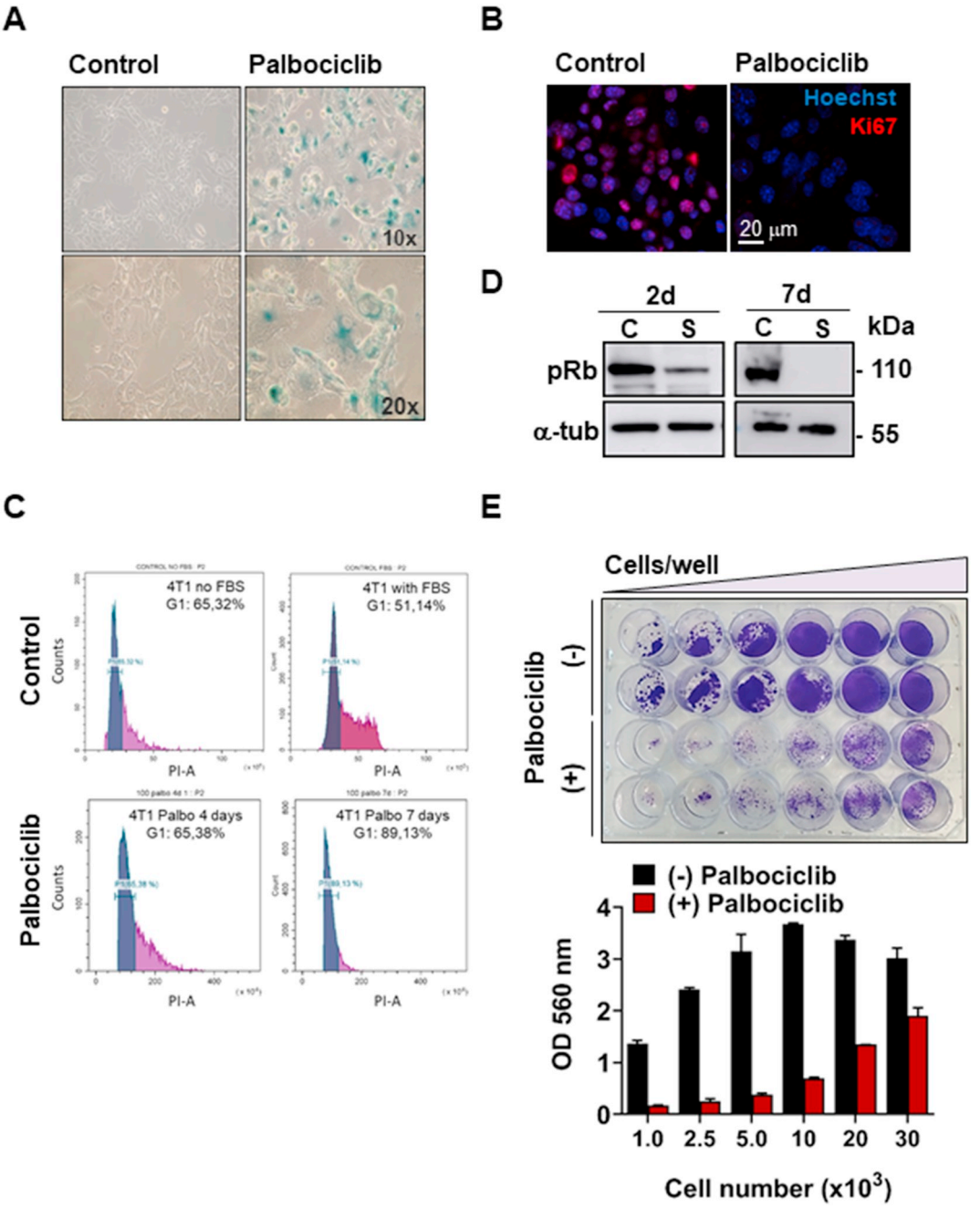

Fig. 1. Palbociclib Induces Senescence in 4 T1 Triple Negative Breast Cancer Cells. A) β-galactosidase activity increases in 4 T1 cells treated with palbociclib. 4 T1 breast cancer cells were treated with 5 μM palbociclib for one week, and senescence induction confirmed by β-galactosidase activity staining assay (blue signal) in senescent 4 T1 cells. B) Decreased Ki67 proliferation marker levels following palbociclib-induced 4 T1 cell senescence. Confocal microscopy immunofluorescence images show staining of Ki67 (red) and nuclei stained with Hoechst (blue). C) 4 T1 cells accumulates in cell cycle G1-phase after 4 and 7 days of palbociclib treatment. Propidium iodide (PI) staining of 4 T1 cells cultured without serum (FBS), in 10% FBS or treated with 5 μM palbociclib for 4 and 7 days. D) pRb decreases upon palbociclib treatment. 4 T1 cells were treated with 5 μM palbociclib and total protein extracts obtained at days 2 and 7 for Western blot analysis of phosphorylated retinoblastoma protein (pRb) (expected band at 110 kDa) with Tubulin used as a loading control. E) 4 T1 cells treated with palbociclib become cell cycle arrested. Cell proliferation studies of control and one-week palbociclib-treated 4 T1 cells. Increasing cell concentrations were seeded in different 24-plate wells (1000, 2500, 5000, 10,000, 20,000, and 30,000; from left to right) and were cultured for one week. Cell cycle arrest was confirmed by crystal violet staining (Left). Graph represents the quantification of violet color by absorbance at 560 nm (right).

cytometry using the membrane-permeable dye JC-1 [60]. JC-1 accumulates in the mitochondria in a potential-dependent manner, shifting the fluorescence emission maximum from green to red. A decrease in the population of cells with a high red/green fluorescence ratio indicates a loss of mitochondrial functionality. A reduction in mitochondrial membrane potential upon navitoclax treatment in palbociclib-induced senescent 4 T1 cells was observed when compared to control 4 T1 cells (Fig. 2B), a finding that agrees with other reported studies of senescent cells [61–63]. Additionally, the treatment of senescent 4 T1 cells with navitoclax led to a further decrease in mitochondrial potential (Fig. 2B) and the selective induction of cell death as measured by the decrease in ATP levels (Fig. 2C). While we ascertained an IC50 value of 0.3 μM for navitoclax in senescent 4 T1 cells, navitoclax exposure only induced cell death in control 4 T1 cells at

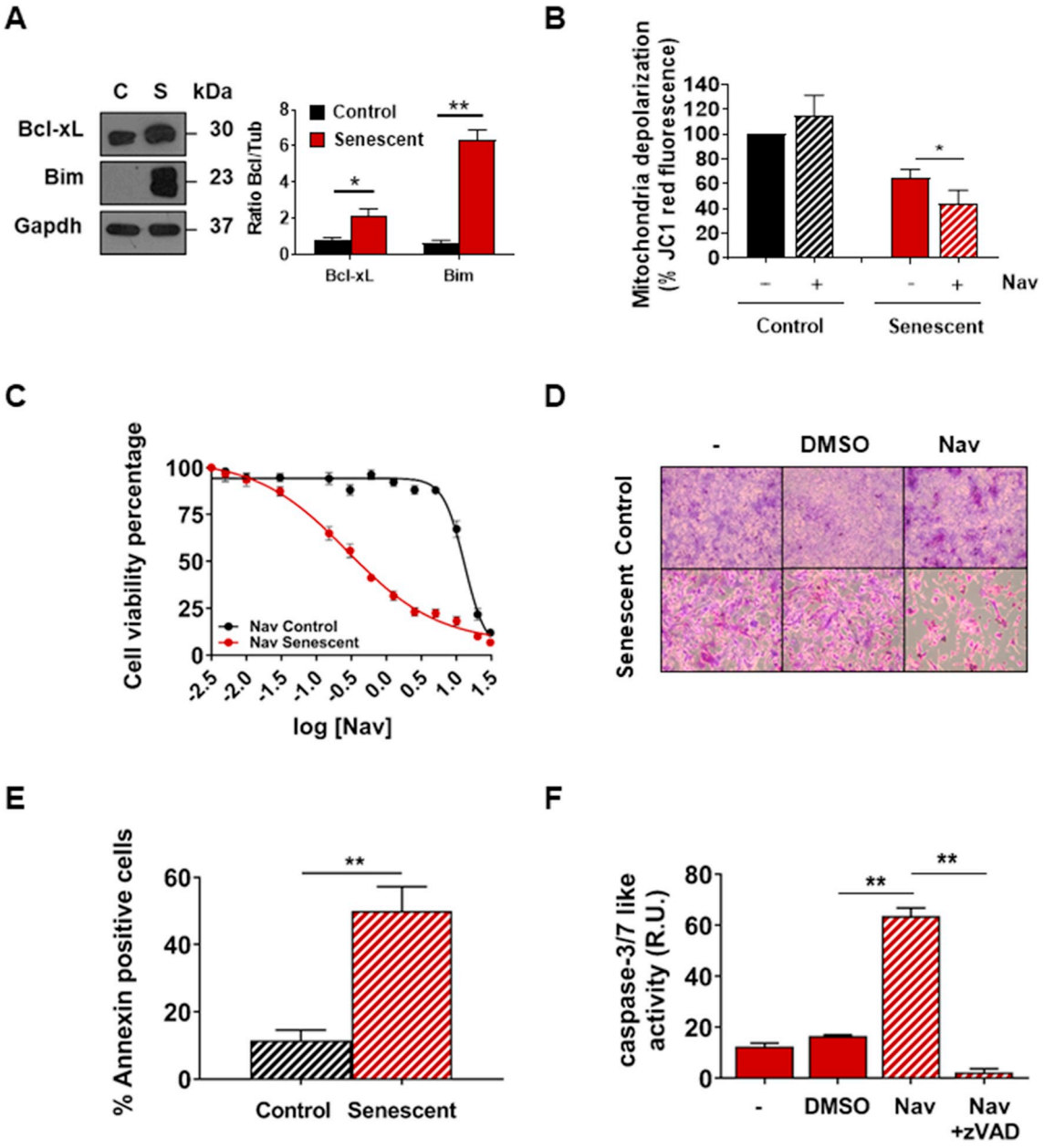

Fig. 2. Navitoclax Treatment Induces Senolysis in Palbociclib-induced senescent 4 T1 Cells. A) Anti-apoptotic Bcl-xL protein is over-expressed in palbociclib treated cells. Bcl-2 family protein expression profile in control and senescent 4 T1 cells analyzed by Western blot (left panel). Quantification of the bands using Gapdh as a loading control ($n = 4$) (right panel). Values are expressed as mean ± SEM, with statistical significance assessed by two-tailed Student's *t*-test: $*p < .05$, $**p < .01$. B) Navitoclax treatment produces depolarization of mitochondria in 4 T1 senescent cells. Red fluorescence analysis of the JC-1 probe was used to measure mitochondria depolarization in control and senescent 4 T1 cells in response to navitoclax treatment ($n = 3$). Values are expressed as mean ± SEM, with statistical significance assessed by two-tailed Student's *t*-test: $*p < .05$. C) Navitoclax induces cell death in palbociclib-induced senescent cells. Control and senescent 4 T1 cells were treated with varying concentrations of navitoclax (0.005 to 30 μM) and cell viability measured after 72 h of treatment by luminescent ATP detection ($n = 6$). D) Selective elimination of palbociclib-induced senescent 4 T1 cells by navitoclax analyzed by crystal violet staining. Cells were treated with navitoclax at the IC_{50} concentration (0.3 μM) for 72 h. E) Treatment of palbociclib-induced senescent 4 T1 cells with navitoclax induces the accumulation of annexin V-positive apoptotic cells. Flow cytometric analysis of Annexin V staining in cells previously treated with navitoclax at the IC_{50} concentration (0.3 μM) for 72 h. Values expressed as mean ± SEM, with statistical significance assessed by two-tailed Student's *t*-test: $**p < .01$. F) Navitoclax treatment induces apoptosis in palbociclib-induced senescent 4 T1 cells. Caspase 3/7 activity measured under the described conditions in the presence or absence of the caspase inhibitor zVAD. Values from three independent experiments expressed as mean ± SEM, with statistical significance assessed by two-tailed Student's *t*-test: **p < .01.

much higher concentrations (Fig. 2C). We also observed a decrease in colony number at IC50 concentrations by crystal violet cell assays (Fig. 2D) and an increase in cell death in Annexin V FITC binding assay by flow cytometry (Fig. 2E). Both studies suggest that navitoclax selectively induced cell death in senescent 4 T1 cells. Finally, we established the apoptotic cell death of 4 T1 cells following exposure to navitoclax *via* caspase 3/7 activity detection assays. The protease activity induced by navitoclax was inhibited by treatment with the caspase inhibitor zVAD (Fig. 2F).

2.3. Oligosaccharide-capped nanoparticles deliver their cargo to senescent 4 T1 cells

To allow therapeutic targeting and the avoidance of off-target

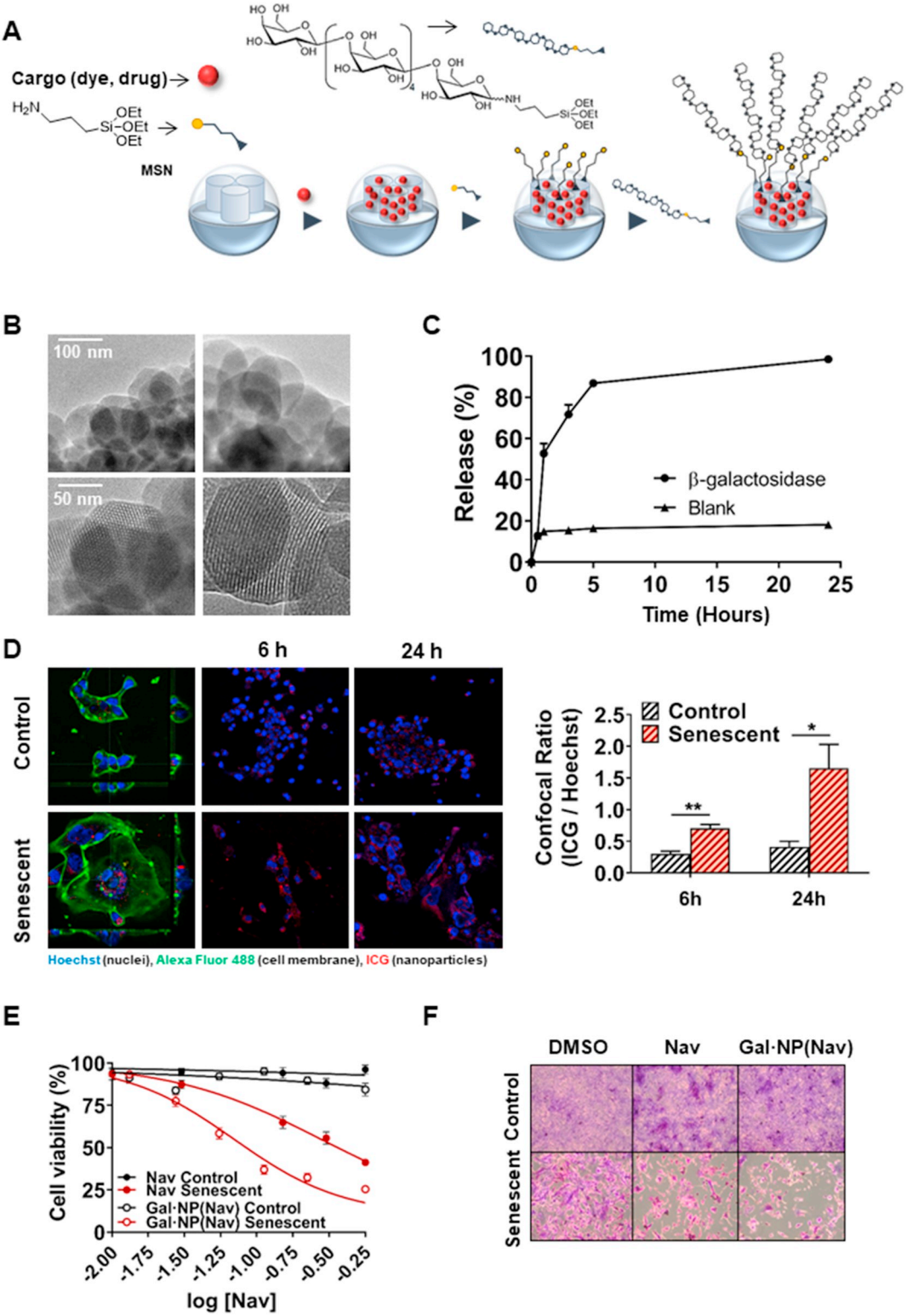

Fig. 3. Capped Nanoparticles Selectively Release their Cargo in a β-galactosidase-dependent Manner. A) Schematic representation of the synthesis of capped mesoporous silica nanoparticles loaded with the cargo (either ICG or navitoclax). Once loaded, the nanoparticles are functionalized on their external surface with (3-aminopropyl) triethoxysilane and the galactooligosaccharide subsequently covalently grafted onto the outer surface of the nanoparticles through the formation of a hemiaminal bond. B) Representative high-resolution TEM images of Gal·NP nanoparticles. Spherical particles of approximately 100 nm with a honeycomb structure of the porous scaffold or channels as black and white longitudinal stripes are observed. Scale bar: 50 nm (lower figures), 100 nm (upper figures). C) Cargo release studies of Gal·NP(ICG) nanoparticles measured by absorption emission spectrometry. Graph depicts cargo release profiles in the absence (blank) and the presence of *Aspergillus oryzae* β-galactosidase in water at pH 4.5 at room temperature at the indicated time points. D) Gal·NP(ICG) nanoparticles internalize preferentially in senescent 4 T1 cells. Confocal analysis of control and senescent cells incubated with the fluorophore-loaded nanoparticles for 6 or 24 h. Blue: Hoechst; Green: WGA Alexa Fluor 488 Conjugate; Red: ICG. Values on the graph (left) derived from confocal imaging expressed as mean ± SEM, with statistical significance assessed by two-tailed Student's *t*-test: $*p < .05$, $**p < .01$. E–F) Treatment of palbociclib-induced senescent 4 T1 cells with Gal·NP(Nav) nanoparticles induces cell death. Cell viability studies of free or encapsulated navitoclax by E) luminescent ATP detection assay in response to increasing concentrations, or F) crystal violet assay at the free navitoclax IC50 concentration (0.3 μM). (For interpretation of the references to color in this figure legend, the reader is referred to the web version of this article.)

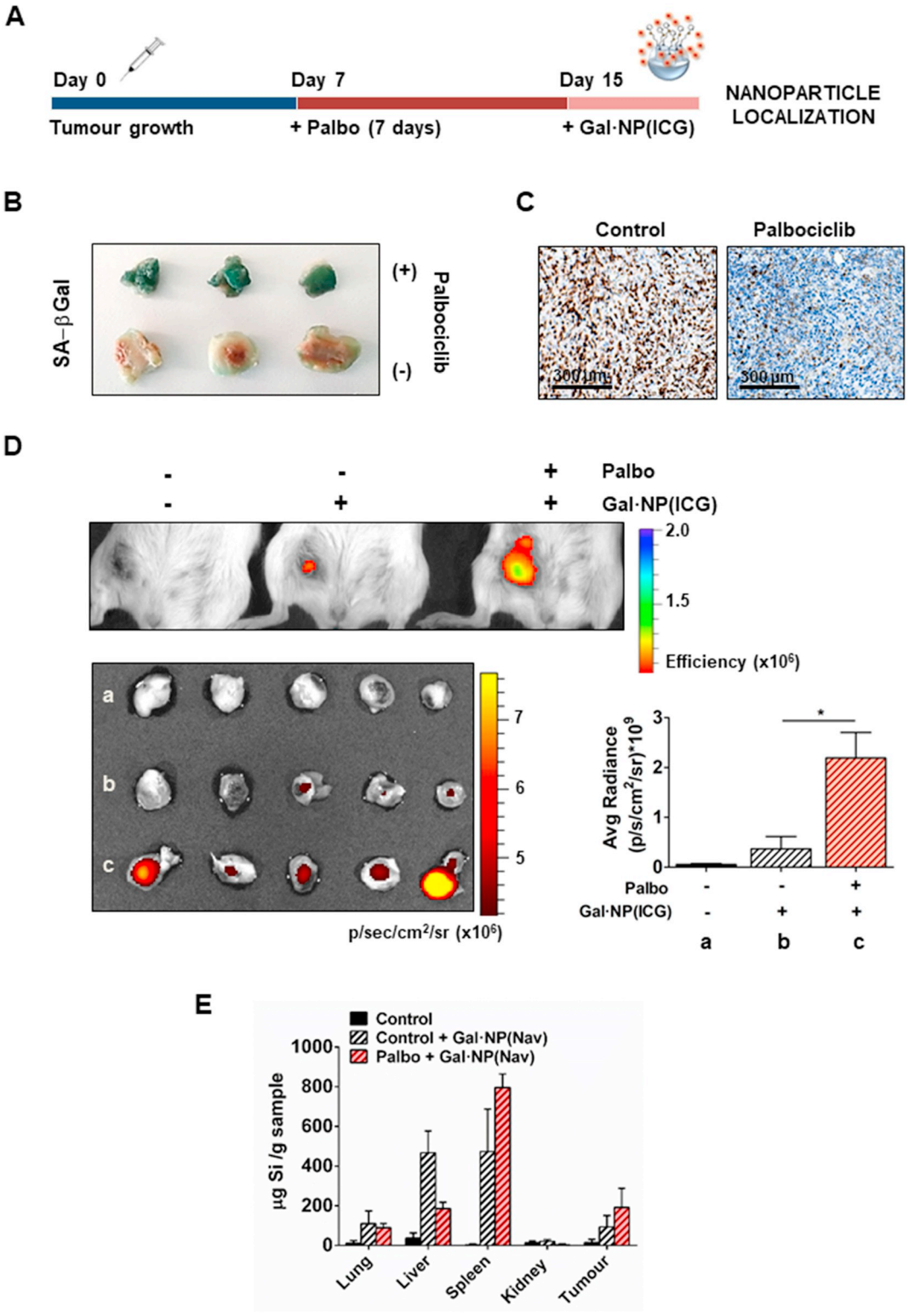

Fig. 4. *In vivo* Induction of Senescence in a TNBC Mouse Model by Palbociclib and Senescent Cell Targeting with Oligosaccharide-capped Nanoparticles. A) Scheme of palbociclib treatment in the TNBC mouse model used to evaluate the induction of senescence. Tumors were grown for one week after orthotopic cell injection and palbociclib treatment then administered by oral gavage (50 mg/kg) for 7 days. Gal·NP(ICG) nanoparticles were intraperitoneally injected (100 mg Gal·NP(ICG)/kg), and animals examined using the IVIS spectrum imaging system at 24-h post-administration to evaluate nanoparticle localization. B) Palbociclib induces senescence in TNBC tumors induced by 4 T1 cell implantation. β-galactosidase staining of breast tumors at the experimental endpoint with and without palbociclib treatment (blue). C) Decrease in Ki67 proliferation marker levels in palbociclib-treated TNBC tumors. Immunohistochemical detection of Ki67 in sections of tumors at the experimental endpoint with and without palbociclib treatment. Scale bar 300 µm. D) Gal·NP(ICG) nanoparticles selectively release their cargo in the tumors of palbociclib-treated TNBC model mice. *In vivo* and *ex vivo* analysis by IVIS spectrum imaging 24 h post-injection. The upper panel shows *in vivo* images from IVIS, while the lower panel (left) shows the *ex vivo* fluorescence signal in tumors and (right) the corresponding emitted fluorescence quantification by Living Image® 4.3.1 software. Values ($n = 5$) expressed as mean ± SEM, with statistical significance assessed by the two-tailed Student's *t*-test: $^*p < .05$.E) Biodistribution of the Gal·NP (ICG) nanoparticles. Silicon levels analyzed by Inductively Coupled Plasma Mass Spectroscopy (ICP-MS). Data expressed as mean ± SEM and represented as µg Si per g of sample.

effects, we next encapsulated navitoclax in MSNs capped with a hexagalactooligosaccharide molecule, thereby generating Gal·NP(Nav) nanoparticles (Fig. 3A). Additionally, we generated similar capped nanoparticles loaded with the fluorescent dye indocyanine green (ICG), referred to as Gal·NP(ICG) nanoparticles. As high levels of lysosomal β-galactosidase activity (SA-βGal) characterize senescent cells, a galactooligosaccharide cap should act as a "molecular gate" that will be specifically hydrolyzed in senescent cells, thereby targeting the release of the navitoclax cargo to the required site of action and avoiding systemic release and the associated side-effects.

Transmission electron microscopy (TEM) imaging of the developed nanoparticles revealed spherical particles of approximately 80–100 nm in diameter, in which the channels of the mesoporous matrix can be visualized as alternate black and white stripes or as a porous honeycomb structure (Fig. 3B, Fig. S3). N_2 adsorption-desorption studies confirmed the presence of uniform cylindrical mesoporous in the starting MSNs with a pore size of 2.8 nm and a total specific surface area of 1091 $m^2\ g^{-1}$ (Table S1). The significant decrease in the adsorbed N_2 volume and surface area observed in loaded Gal·NP(ICG) nanoparticles (57 $m^2\ g^{-1}$) confirmed cargo loading (Fig. S4).

Dynamic light scattering (DLS) measurements (Fig. S5) revealed a hydrodynamic diameter for the starting MSNs and final Gal·NP(ICG) nanoparticles of 183 nm and 376 nm, respectively (Table S2), with a single population distribution indicating the uniformity of the nanoparticle population. An increase in the hydrodynamic diameter, as well as an increase in zeta potential values, are consistent with the external functionalization of the nanoparticles with galactooligosaccharides; of note, similar alterations in these parameters occurred for capped nanoparticles without cargo (Gal·NP(0) - 249 nm) and in capped nanoparticles carrying cargo (Gal·NP(Nav) - 301 nm).

Moreover, experiments with Gal·NP(ICG) and Gal·NP(Nav) nanoparticles demonstrated efficient cargo capping and selective release in the presence of fungal β-galactosidase, which hydrolyzes the galactooligosaccharide cap (Fig. S6 and Fig. 3C, respectively). For Gal·NP (Nav) nanoparticles, thermogravimetric and high-performance liquid chromatography (HPLC) analyses indicated 141.4 mg of galactooligosaccharides per gram of nanoparticle and the delivery of 60 mg of navitoclax per gram of nanoparticle in the presence of β-galactosidase.

We validated Gal·NP(ICG) nanoparticles in control and senescent 4 T1 cells by confocal microscopy and flow cytometry; both studies demonstrated that Gal·NP(ICG) nanoparticles released their content (the ICG dye) more efficiently in palbociclib-induced senescent 4 T1 cells (high β-galactosidase activity) than in control 4 T1 cells (low β-galactosidase activity) after 6 or 24 h (Fig. 3D, Fig. S7). The discovery of the ICG dye located in a perinuclear region suggests the release of the drug in the lysosomal compartment (Fig. 3D).

We next evaluated Gal·NP(Nav) nanoparticles, finding that treatment of control and senescent 4 T1 cells with increasing concentrations of Gal·NP(Nav) caused a selective decrease in senescent cell viability with an IC50 of 0.07 μM for Gal·NP(Nav), a value significantly lower than that obtained for the free form of the drug (0.3 μM) (Fig. 3E). Crystal violet staining of cells treated with Gal·NP(Nav) at the IC50 concentration value of free navitoclax confirmed the selective induction of cell death in senescent cells (Fig. 3F). Finally, biocompatibility studies employing capped nanoparticles with no cargo (Gal·NP(0)) demonstrated that empty nanoparticles failed to induce cytotoxic effects in control or senescent 4 T1 cells at 72 h for all studied concentrations (Fig. S8).

In summary, we demonstrated that oligosaccharide-capped nanoparticles preferentially deliver ICG to senescent 4 T1 cells. Furthermore, navitoclax displayed enhanced senolytic activity when encapsulated within oligosaccharide-capped nanoparticles, demonstrating the efficacy of this encapsulation approach.

2.4. *In vivo* analysis of triple negative breast cancer treatment with senescence-inducing chemotherapy and nanotherapeutic-mediated senolysis

Following *in vitro* validation of the nanoparticles, we next studied the combination of senogenesis (senoinduction by palbociclib) with targeted senolysis (using Gal·NP(Nav) or free navitoclax) in an orthotopic TNBC mouse model, aiming for improved antitumor efficacy.

We injected 4 T1 cells into the mammary pads of Balb/cByJ female mice (4–6 weeks) to induce tumor formation, and after one week of tumor growth, mice were treated with palbociclib by daily oral gavage for a further week (50 mg/kg) (Fig. 4A). Senescence was efficiently induced in palbociclib treated animals, as evidenced by the increase in SA-βGal activity in tumors (Fig. 4B) and the immunohistochemical detection of reduced levels of Ki67 in tumor sections (Fig. 4C).

Gal·NP(ICG) nanoparticles were intraperitoneally administrated after one week of palbociclib treatment to evaluate their ability to specifically release cargo in senescent cells (Fig. 4A). *In vivo* imaging studies of probe distribution at 24 h post-injection demonstrated the preferential accumulation of ICG in palbociclib-treated 4 T1 tumors (Fig. 4D) with only a weak fluorescent signal above background observed in tumors of animals not treated with palbociclib. The biodistribution of nanoparticles was studied by the determination of silicon levels in various organs by inductively coupled plasma mass spectroscopy (ICP-MS) (Fig. 4E). Interestingly, the levels of silicon detected indicated that nanoparticles accumulated both in senescent and non-senescent tumors; therefore, the enhanced fluorescent signal in palbociclib-treated tumors derives from β-galactosidase-induced cargo release from Gal·NP(ICG). Of note, the ICG remains strongly auto-quenched inside the capped nanoparticles [43–45]. While these findings provide proof of principle for nanotherapy-mediated targeting of cargos to senescent tumor cells, they also support the application of Gal·NP (ICG) in the *in vivo* detection of senescent cells *via* optical imaging.

After confirming that galactooligosaccharide-capped nanoparticles can selectively release their cargo within senescent tumor cells *in vivo*, we next evaluated navitoclax-loaded nanoparticles (Gal·NP(Nav)) in the same system. In this case, to have an appropriate therapeutic window to study the effectivity of co-treatments we treated mice with palbociclib three days after the orthotopic injection 4 T1 cells, and one day after initiating palbociclib administration, we administered free navitoclax or Gal·NP(Nav) nanoparticles for 15 days. Tumor size and body weight was measured every two days to evaluate treatment efficacy and safety (Fig. 5A). Animals receiving palbociclib displayed significantly reduced tumor sizes when compared with non-palbociclib treated groups (Fig. 5B). Tumor size reduction by palbociclib is of particular interest, as on-going clinical trials with palbociclib in combination with bicalutamide in TNBC patients focus on patients overexpressing the androgen receptor (AR) (Clinical Trial ID: NCT02605486) (55). The 4 T1 cell line does not express the AR receptor (Fig. S9), so the observed antitumoral activity of palbociclib in the 4 T1 TNBC mouse model suggests the potential application of this drug to novel TNBC patient subgroups, and provides evidence for the need to search for new biomarkers. While the treatment of TNBC model mice with Gal·NP(Nav) nanoparticles only failed to induce a reduction in tumor size, treatment of mice with both palbociclib and Gal·NP(Nav) nanoparticles prompted a robust therapeutic effect with a significant decrease in tumor size, thereby demonstrating that the therapeutic effect of Gal·NP(Nav) nanoparticles requires the induction of senescence (Fig. 5B–C and Fig. S10). In addition, while animals treated with combination palbociclib plus free navitoclax showed weight loss, all palbociclib and Gal·NP (Nav) nanoparticle treated animals survived until the end of the experiment without significant alterations to body weight (Fig. S11).

Of note, groups not treated with the CDK4/6 inhibitor (Control, Nav, or Gal·NP(Nav)) reached the humane endpoint at 15 days tumor-induction and were sacrificed (Fig. 5D and Fig. S11). Treatment of tumor-bearing animals with navitoclax in the absence of palbociclib did not lead to significant reductions in tumor size or weight loss (Fig. 5B

and C), and these mice also had to be sacrificed before the experimental endpoint (Fig. 5D). Importantly, the combination of palbociclib and free navitoclax treatment led to reduced tumor growth (Fig. 5C); however, animals had to be euthanized before the endpoint of the study due to excessive weight loss (more than 10%) (Fig. 5D and Fig. S11) suggesting that the encapsulation of navitoclax effectively reduces associated systemic toxicity. Moreover, animals treated with the combination of palbociclib and free navitoclax showed a significant reduction in the number of platelets. This toxicity was partially alleviated in the group of animals receiving palbociclib plus Gal·NP(Nav) (Fig. S12 and S13).

We also studied lung metastasis, given its frequent occurrence in TNBC patients; encouragingly, we established that treatment of TNBC model mice with palbociclib and Gal·NP(Nav) nanoparticles prompted a

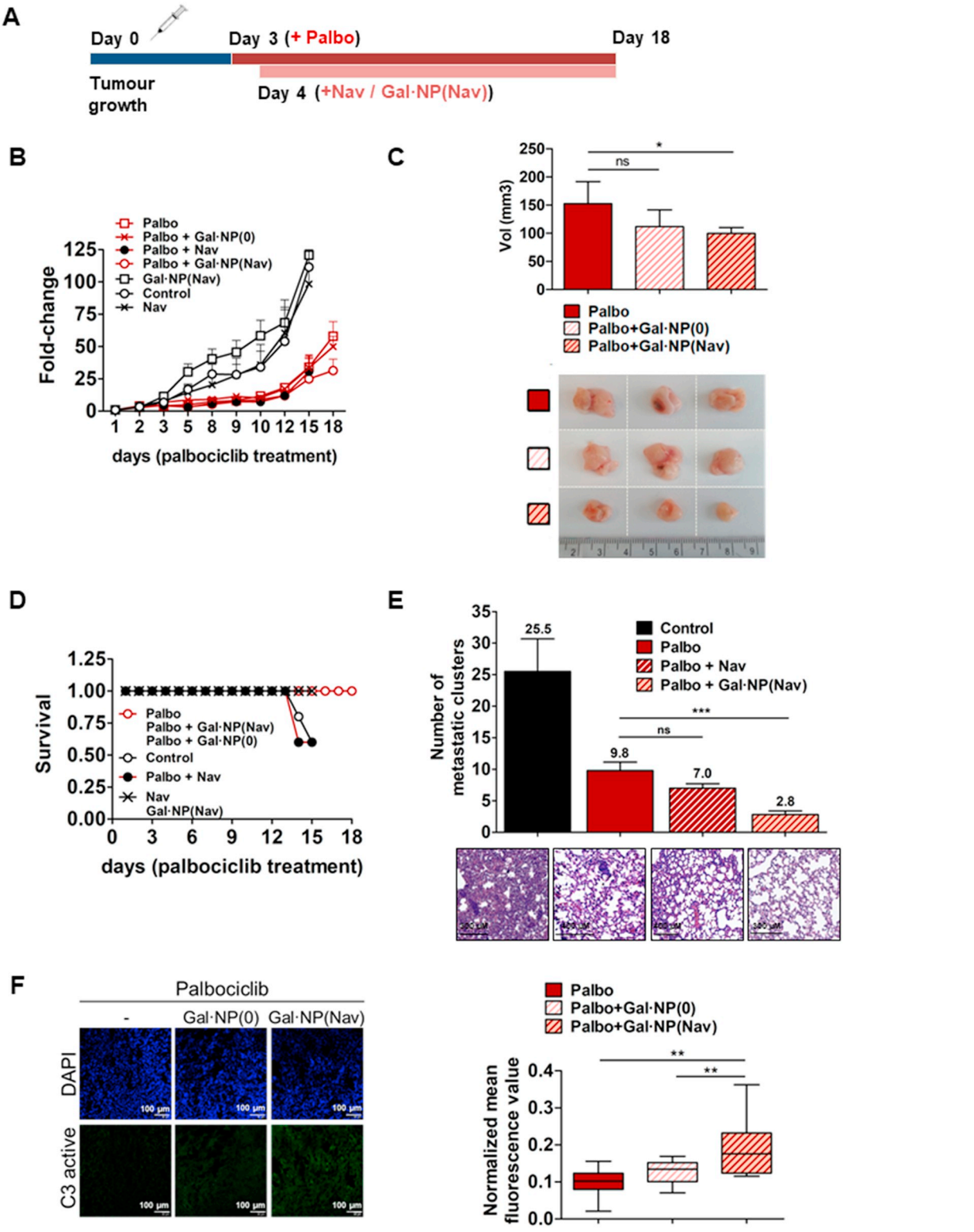

(caption on next page)

Fig. 5. Senolysis Induced by Gal·NP(Nav) Nanoparticles Effectively Reduces Tumor Size. A) Schema of palbociclib treatment in the TNBC mouse model combined with senolytic treatment with free or encapsulated navitoclax. Three days after orthotopic 4 T1 cell injection, daily palbociclib treatment started and was maintained for 17 days (oral gavage, 100 mg/kg). One day after palbociclib initiation, daily senolytic treatment started and was maintained for 16 days (free navitoclax: oral gavage, 25 mg/kg; Gal·NP(Nav): intraperitoneal injection, 40 mg Gal·NP(Nav)/kg (equivalent to 2.5 mg/kg = free Navitoclax). B) Combination treatment of palbociclib with Gal·NP(Nav) nanoparticles reduces TNBC tumor growth. Balb/cByJ female mice were orthotopically injected with 4 T1 breast cancer cells and treated daily with vehicle or palbociclib and free navitoclax or Gal·NP(Nav) alone or in combination at the indicated doses in A). For each tumor, the relative volume change was calculated in comparison to its baseline before treatment. Values ($n = 5$) are expressed as mean ± SEM. In the case of palbociclib plus navitoclax, control and navitoclax groups the last time points are ($n = 3$) due to animal loss. C) Volumes for selected treatment approaches (palbociclib alone, palbociclib combined with empty nanoparticles (Gal·NP(0)), and palbociclib combined with encapsulated navitoclax (Gal·NP(Nav)) at experimental endpoint expressed in mm^3 as mean ± SEM (n = 5), and statistical significance was assessed by One-way ANOVA: $*p < .05$. The image depicts representative tumor samples. D) Encapsulation of navitoclax enhances the survival of TNBC model mice. Kaplan-Meier curve during the experimental period in response to the indicated treatments. E) Combined palbociclib and Gal·NP(Nav) nanoparticle treatment reduces lung metastases in the TNBC mouse model. Metastatic cell clusters were counted in lung hematoxylin-eosin stained sections. Scale bar correspond to 300 μm. Data plotted in the associated graph (n = 5). Values represented as mean ± SEM, with statistical significance assessed by One-way ANOVA: $***p < .001$. F) Caspase 3 activity induction in tumors of palbociclib and Gal·NP(Nav) nanoparticle treated TNBC model mice. Representative images of active caspase-3 immunofluorescence (left panel; scale bar 50 μm) and mean fluorescence quantification (right panel) in tumor sections. Statistical significance assessed by One-way ANOVA: $**p < .01$.

highly significant reduction in the number of lung metastases when compared to mice treated with palbociclib only (Fig. 5E). In addition to immunohistochemical studies, we evaluated lung metastases using India ink inflation of tumor-bearing lungs and also by colonoy formation assays in explanted cells. The selection of the 4 T1 model provided us the opportunity to culture metastatic cells in the presence of 6-thioguanine (6-TG). Interestingly, treatment with the Gal·NP(Nav) nanoparticle decreases lung metastases (Fig. S14).

Finally, assessment of apoptotic cell death by the immunofluorescent detection of active caspase 3 in tumor sections from treated mice (Fig. 5F) suggested that Gal·NP(Nav) nanoparticles administration to palbociclib-treated TNBC model mice significantly induced senolysis in tumors *in vivo* when compared to palbociclib treatment alone or palbociclib treatment combined with empty nanoparticles.

Collectively, these data demonstrate that encapsulation of the senolytic drug navitoclax can inhibit TNBC development and metastasis *in vivo* following palbociclib treatment while also inhibiting unwanted systemic side-effects.

3. Discussion

Senescence has been traditionally considered an evolutionary strategy to avoid tumor proliferation [64]. Based on this assumption, antitumoral senescence inducing agents have evolved and reached application in the clinic. However, the advancement and evolution of our knowledge regarding cancer had provided evidence that senescence represents a double-edged sword. Recent reports have established that traditional chemotherapeutics, such as doxorubicin, and radiotherapy induce cell senescence in tumors [3], but this therapy-induced senescence can have both positive and negative consequences for patients; while macrophages eliminate senescent cells and contribute to the generation of anti-tumoral immune responses, senescent cells also represent a source of pro-inflammatory signaling that induces a pro-tumorigenic microenvironment that supports tumor development.

A seminal study showed that genetic clearance of p16INK4A-expressing senescent cells increased the survival of tumor-bearing mice [65]; since the publication of this study, numerous studies have found that the elimination of senescent cells can reverse disease-associated phenotypes in mouse models [32,66–69,70,71]. However, these studies have yet to adequately address how the dual behavior of senescence could affect treatments that induce senescence in tumors that are currently in clinical use, such as the CDK4/6 inhibitor palbociclib. Considering these circumstances, there exists a clear potential for treatment improvement, and in this study, we have demonstrated that a combination of senogenesis (senoinduction with palbociclib) with nanotherapy-targeted senolysis (encapsulated navitoclax) in an orthotopic TNBC mouse model improves antitumor efficacy and reduced both metastasis and navitoclax off-target toxicity. This aggressive mouse model recapitulates many of the critical characteristics of human TNBC [49–52], making the results obtained from this study particularly relevant.

In terms of palbociclib treatment, we demonstrated that treatment with the CDK4/6 inhibitor palbociclib efficiently induced senescence in the 4 T1 TNBC cell line, which does not express the AR. Pabociclib produces changes in mitochondrial potential a common characteristic of senescent cells that contributes not only to the establishment of the senescent phenotype but also to the sensitization to senolytic drugs [72].

As stated previously, on-going clinical trials with palbociclib in TNBC patients mainly focus on patients overexpressing AR. This study further supports the potential application of palbociclib to other subgroups of TNBC or other types of tumors, independently from the AR-state, since several molecular factors contribute to the response and level of sensitivity to CDK4/6 treatment. However, a lot of work needs to be done in the scientific community, to identify the biomarker for an appropriate selection of patients which are suitable for CDK4/6 inhibitors-based treatment. We also prepared capped nanoparticles loaded with the fluorescent dye indocyanine green, Gal·NP(ICG), and used them to demonstrate that these nanoparticles released their content more efficiently in palbociclib-induced senescent 4 T1 cells compared to control cells, in concordance with their high levels of β-galactosidase activity. Moreover, the treatment of palbociclib-induced senescent 4 T1 cells with Gal·NP(Nav) induce a selective decrease in cell viability to a level lower than that found for the free navitoclax. Furthermore, *in vivo* imaging studies of Gal·NP(ICG) distribution 24 h post-injection established the preferential accumulation of fluorescent dye in palbociclib-treated tumors, thereby demonstrating that our nanoparticles can be of use for the detection of senescence by *in vivo* imaging.

Importantly, Gal·NP(Nav) nanoparticles provide a therapeutic benefit when combined with palbociclib; tumor-bearing mice treated in this manner survived to the experimental endpoint without significant changes in body weight, whereas treatment with palbociclib in combination with free navitoclax led to reduced survival and significant weight loss in surviving animals which required them to be sacrificed before the experimental endpoint. Additionally, TNBC model mice treated with palbociclib and Gal·NP(Nav) present fewer lung metastases when compared to mice treated with palbociclib only, a remarkable result in terms of long-term prognosis and survival.

The reduction of tumor size observed upon senolysis could be explained in different terms: i) the immune surveillance system is overloaded as consequence of continuous palbociclib induced senescence, and the senolytic drug helps to eliminate senescent cells; ii) chronically induced senescent cells actively evade the immune system and senolysis represents an alternative contribution to their elimination; iii) senolysis acts as an adjuvant therapy activating immune surveillance and favoring senescent cells elimination. However, the extent to which these mechanisms contribute to tumor reduction remains to be elucidated.

Further studies addressing these questions could contribute to outline new antitumor strategies.

Acknowledgments

The M.O. laboratory members thank the financial support from the Spanish Government (project SAF2017-84689-R (MINECO/AEI/FEDER, EU)) and the Generalitat Valenciana (project PROMETEO/2019/065). The R.M. laboratory members thank the financial support from the Spanish Government (projects RTI2018-100910-B-C41 and RTI2018-101599-B-C22 (MCUI/FEDER, EU) and the Generalitat Valenciana (project PROMETEO 2018/024). Both I.G. and B.L-T. are grateful to the Generalitat Valenciana and the Spanish Ministry of Economy, respectively, for their Ph.D. grants. I.G. would like to thank I. Borreda and J. Forteza and the Instituto Valenciano de Patología for their special collaboration and F. Sancenón for his appreciated help.

Declaration of Competing Interest

R.M. and M.S. are co-founder and shareholder of Senolytic Therapeutics, Inc. (USA) and Senolytic Therapeutics, S.L. (Spain).

Appendix A. Supplementary data

Supplementary data to this article can be found online at https://doi.org/10.1016/j.jconrel.2020.04.045.

References

[1] A. Hernandez-Segura, J. Nehme, M. Demaria, Hallmarks of cellular senescence, Trends Cell Biol. 28 (6) (2018) 436–453.
[2] L. Hayflick, P.S. Moorhead, The serial cultivation of human diploid cell strains, Exp. Cell Res. 1 (January) (1961).
[3] J.C. Acosta, J. Gil, Senescence: a new weapon for cancer therapy, Trends Cell Biol. 22 (4) (2012) 211–219.
[4] C.J. Sieben, I. Sturmlechner, B. van de Sluis, J.M. van Deursen, Two-step senescence-focused cancer therapies, Trends Cell Biol. 28 (9) (2018) 723–737.
[5] J.W. Goldman, P. Shi, M. Reck, L. Paz-Ares, A. Koustenis, K.C. Hurt, Treatment rationale and study design for the JUNIPER study: a randomized phase III study of abemaciclib with best supportive care versus erlotinib with best supportive care in patients with stage IV non-small-cell lung cancer with a detectable KRAS mutation whose disease has progressed after platinum-based chemotherapy, Clin. Lung Cancer 17 (1) (2016) 80–84.
[6] R.S. Finn, J. Dering, D. Conklin, O. Kalous, D.J. Cohen, A.J. Desai, et al., PD 0332991, a selective cyclin D kinase 4/6 inhibitor, preferentially inhibits proliferation of luminal estrogen receptor-positive human breast cancer cell lines in vitro, Breast Cancer Res. 11 (5) (2009) 1–13.
[7] B. Geoerger, F. Bourdeaut, S.G. DuBois, M. Fischer, J.I. Geller, N.G. Gottardo, et al., A phase I study of the CDK4/6 inhibitor ribociclib (LEE011) in pediatric patients with malignant rhabdoid tumors, neuroblastoma, and other solid tumors, Clin. Cancer Res. 23 (10) (2017) 2433–2441.
[8] D. Kwapisz, Cyclin-dependent kinase 4/6 inhibitors in breast cancer: palbociclib, ribociclib, and abemaciclib, Breast Cancer Res. Treat. 166 (1) (2017) 41–54.
[9] S. Pernas, S.M. Tolaney, E.P. Winer, S. Goel, CDK4/6 inhibition in breast cancer: current practice and future directions, Ther. Adv. Med. Oncol. 10 (2018) 1–15.
[10] R.L. Sutherland, E.A. Musgrove, CDK inhibitors as potential breast cancer therapeutics: new evidence for enhanced efficacy in ER + disease, Breast Cancer Res. 11 (6) (2009) 2–3.
[11] D.W. Fry, P.J. Harvey, P.R. Keller, W.L. Elliott, M. Meade, E. Trachet, et al., Specific inhibition of cyclin-dependent kinase 4/6 by PD 0332991 and associated antitumor activity in human tumor xenografts, Mol. Cancer Ther. 3 (11) (2004) 1427–1438.
[12] J.A. Beaver, L. Amiri-Kordestani, R. Charlab, W. Chen, T. Palmby, A. Tilley, et al., FDA approval: Palbociclib for the treatment of postmenopausal patients with estrogen receptor-positive, HER2-negative metastatic breast cancer, Clin. Cancer Res. 21 (21) (2015) 4760–4766.
[13] R. Finn, J. Crown, I. Lang, K. Boer, Oncology IB-T lancet, 2015 U, The cyclin-dependent kinase 4/6 inhibitor palbociclib in combination with letrozole versus letrozole alone as first-line treatment of oestrogen receptor-positive, HER2-negative, advanced breast cancer (PALOMA-1/TRIO-18): a randomised phase 2 study, Elsevier (2015) 1.
[14] J.W. Chiu, G. Kwok, T. Yau, R. Leung, Editorial to “Palbociclib and letrozole in advanced breast cancer.”, Transl. Cancer Res. 6 (S2) (2017) S376–S379.
[15] T. Traina, K. Cadoo, A. Gucalp, Palbociclib: an evidence-based review of its potential in the treatment of breast cancer, Breast Cancer Targets Ther. 6 (2014) 123.
[16] N.C. Turner, J. Ro, F. André, S. Loi, S. Verma, H. Iwata, et al., Palbociclib in hormone-receptor–positive advanced breast cancer, N. Engl. J. Med. 373 (3) (2015) 209–219.
[17] M. Cristofanilli, N.C. Turner, I. Bondarenko, J. Ro, S.A. Im, N. Masuda, et al., Fulvestrant plus palbociclib versus fulvestrant plus placebo for treatment of hormone-receptor-positive, HER2-negative metastatic breast cancer that progressed on previous endocrine therapy (PALOMA-3): final analysis of the multicentre, double-blind, phase 3 randomised controlled trial, Lancet Oncol. 17 (4) (2016) 425–439.
[18] S. Lee, C.A. Schmitt, The dynamic nature of senescence in cancer, Nat. Cell Biol. 21 (1) (2019) 94–101.
[19] S. Giaimo, D’Adda di Fagagna F., Is cellular senescence an example of antagonistic pleiotropy? Aging Cell 11 (3) (2012) 378–383.
[20] D. Muñoz-Espín, M. Serrano, Cellular senescence: from physiology to pathology, Nat. Rev. Mol. Cell Biol. 15 (7) (2014) 482–496.
[21] F. Rodier, J. Campisi, Four faces of cellular senescence, J. Cell Biol. 192 (4) (2011) 547–556.
[22] S. He, N.E. Sharpless, Senescence in health and disease, Cell. 169 (6) (2017) 1000–1011.
[23] D. McHugh, J. Gil, Senescence and aging: causes, consequences, and therapeutic avenues, J. Cell Biol. 217 (1) (2018) 1–13.
[24] M. Schosserer, J. Grillari, M. Breitenbach, The dual role of cellular senescence in developing tumors and their response to cancer therapy, Front. Oncol. 7 (November) (2017).
[25] J.A. Ewald, J.A. Desotelle, G. Wilding, D.F. Jarrard, Therapy-induced senescence in cancer, J. Natl. Cancer Inst. 102 (20) (2010) 1536–1546.
[26] M. Demaria, M.N.O. Leary, J. Chang, L. Shao, S. Liu, K. Koenig, et al., Cellular Senescence Promotes Adverse Effects of Chemotherapy and Cancer Relapse, 7(2) (2017), pp. 165–176.
[27] R.R. Gordon, P.S. Nelson, Cellular senescence and cancer chemotherapy resistance, Drug Resist. Updat. 15 (1–2) (2012) 123–131.
[28] E. Wieland, J. Rodriguez-Vita, S.S. Liebler, C. Mogler, I. Moll, S.E. Herberich, et al., Endothelial Notch1 activity facilitates metastasis, Cancer Cell 31 (3) (2017) 355–367.
[29] M. Milanovic, D.N.Y. Fan, D. Belenki, J.H.M. Däbritz, Z. Zhao, Y. Yu, et al., Senescence-associated reprogramming promotes cancer stemness, Nature 553 (7686) (2017) 96–100.
[30] S. Parrinello, Stromal-epithelial interactions in aging and cancer: senescent fibroblasts alter epithelial cell differentiation, J. Cell Sci. 118 (3) (2005) 485–496.
[31] J.L. Kirkland, T. Tchkonia, Y. Zhu, L.J. Niedernhofer, P.D. Robbins, The clinical potential of senolytic drugs, J. Am. Geriatr. Soc. 65 (10) (2017) 2297–2301.
[32] B.G. Childs, M. Gluscevic, D.J. Baker, R.M. Laberge, D. Marquess, J. Dananberg, et al., Senescent cells: an emerging target for diseases of ageing, Nat. Rev. Drug Discov. 16 (10) (2017) 718–735.
[33] B. Lozano-Torres, A. Estepa-Fernández, M. Rovira, M. Orzáez, M. Serrano, R. Martínez-Máñez, et al., The chemistry of senescence, Nat. Rev. Chem. 3 (2019) 426–441.
[34] Y. Zhu, T. Tchkonia, H. Fuhrmann-Stroissnigg, H.M. Dai, Y.Y. Ling, M.B. Stout, et al., Identification of a novel senolytic agent, navitoclax, targeting the Bcl-2 family of anti-apoptotic factors, Aging Cell 15 (3) (2016) 428–435.
[35] E. Wang, Senescent human fibroblasts resist programmed cell death, and failure to suppress bcl2 is involved, Cancer Res. 5585 (112) (1995) 2284–2292.
[36] M.P. Baar, R.M.C. Brandt, D.A. Putavet, J.D.D. Klein, K.W.J. Derks, B.R.M. Bourgeois, et al., Targeted apoptosis of senescent cells restores tissue homeostasis in response to chemotoxicity and aging, Cell 169 (1) (2017) 132–147.e16.
[37] Y. Zhu, T. Tchkonia, T. Pirtskhalava, A.C. Gower, H. Ding, N. Giorgadze, et al., The Achilles’ heel of senescent cells: From transcriptome to senolytic drugs, Aging Cell (March) (2015) 644–658.
[38] J. Chang, Y. Wang, L. Shao, R.-M. Laberge, M. Demaria, J. Campisi, et al., Clearance of senescent cells by ABT263 rejuvenates aged hematopoietic stem cells in mice, Nat. Med. 22 (1) (2015) 78–83.
[39] B.T. Kile, The role of apoptosis in megakaryocytes and platelets, Br. J. Haematol. 165 (2) (2014) 217–226.
[40] E. Aznar, M. Oroval, L. Pascual, J.R. Murguía, R. Martínez-Máñez, F. Sancenón, Gated materials for on-command release of guest molecules, Chem. Rev. 116 (2) (2016) 561–718.
[41] A. Llopis-Lorente, B. Lozano-Torres, A. Bernardos, R. Martínez-Máñez, F. Sancenón, Mesoporous silica materials for controlled delivery based on enzymes, J. Mater. Chem. B 5 (17) (2017) 3069–3083.
[42] F. Sancenón, L. Pascual, M. Oroval, E. Aznar, Gated Silica Mesoporous Materials in Sensing Applications, (2015), pp. 418–437.
[43] M. Vallet-Regí, M. Colilla, I. Izquierdo-Barba, M. Manzano, Mesoporous silica nanoparticles for drug delivery: current insights, Molecules 23 (1) (2018) 1–19.
[44] Y.L. Su, S.H. Hu, Functional nanoparticles for tumor penetration of therapeutics, Pharmaceutics 10 (4) (2018) 1–21.
[45] C. Giménez, C. De La Torre, M. Gorbe, E. Aznar, F. Sancenón, J.R. Murguía, et al., Gated mesoporous silica nanoparticles for the controlled delivery of drugs in cancer cells, Langmuir 31 (12) (2015) 3753–3762.
[46] A. Agostini, L. Mondragón, A. Bernardos, R. Martínez-Máñez, M. Dolores Marcos, F. Sancenón, et al., Targeted cargo delivery in senescent cells using capped mesoporous silica nanoparticles, Angew. Chem. Int. Ed. 51 (42) (2012) 10556–10560.
[47] A. Bernardos, L. Mondragón, E. Aznar, M.D. Marcos, R. Martínez-Máñez, F. Sancenón, et al., Enzyme-responsive intracellular controlled release using nanometric silica mesoporous supports capped with “saccharides.”, ACS Nano 4 (11) (2010) 6353–6368.
[48] D. Muñoz-Espín, M. Rovira, I. Galiana, C. Giménez, B. Lozano-Torres, M. Paez-Ribes, et al., A versatile drug delivery system targeting senescent cells, EMBO Mol. Med. (2018) e9355.
[49] P. Kaur, G.M. Nagaraja, H. Zheng, D. Gizachew, M. Galukande, S. Krishnan, et al., A

mouse model for triple-negative breast cancer tumor-initiating cells (TNBC-TICs) exhibits similar aggressive phenotype to the human disease, BMC Cancer 12 (2012).
[50] W.D. Foulkes, I.E. Smith, J.S. Reis-Filho, Triple-negative breast cancer, N. Engl. J. Med. 363 (20) (2010) 1938–1948.
[51] K. Aysola, A. Desay, C. Welch, et al., Triple negative breast cancer – an overview, Hereditary Genet. (Suppl. 2) (2013).
[52] B.A. Pulaski, S. Ostrand-Rosenberg, Mouse 4T1 breast tumor model, Curr. Protoc. Immunol. 20 (39) (2001), https://doi.org/10.1002/0471142735.im2002s39.
[53] M. Collado, M. Serrano, Senescence in tumors: evidence from mice and humans, Nat. Rev. Cancer 10 (1) (2010) 51–57.
[54] S. Goel, M.J. Decristo, A.C. Watt, H. Brinjones, J. Sceneay, B.B. Li, et al., CDK4/6 inhibition triggers anti-tumour immunity, Nature 548 (7668) (2017) 471–475.
[55] U.S. Asghar, A.R. Barr, R. Cutts, M. Beaney, I. Babina, D. Sampath, et al., Single-cell dynamics determines response to CDK4/6 inhibition in triple-negative breast cancer, Clin. Cancer Res. 23 (18) (2017) 5561–5572.
[56] G.P. Dimri, X. Leet, G. Basile, M. Acosta, G. Scorrt, C. Roskelley, et al., A biomarker that identifies senescent human cells in culture and in aging skin in vivo (replicative senescence/tumor suppression/18-galactosidase), Cell Biol. 92 (September) (1995) 9363–9367.
[57] B.Y. Lee, J.A. Han, J.S. Im, A. Morrone, K. Johung, E.C. Goodwin, et al., Senescence-associated β-galactosidase is lysosomal β-galactosidase, Aging Cell 5 (2) (2006) 187–195.
[58] A. Letai, To prime, or not to prime: that is the question, Cold Spring Harb. Symp. Quant. Biol. 81 (2016) 131–140.
[59] C. Billard, BH3 mimetics: status of the field and new developments, Mol. Cancer Ther. 12 (9) (2013) 1691–1700.
[60] M. Reers, S.T. Smiley, C. Mottola-Hartshorn, et al., Mitochondrial membrane potential monitored by JC-1 dye, Methods Enzymol. 260 (1995) 406–417.
[61] M.M. Sugrue, Y. Wang, H.J. Rideout, R.M.E. Chalmers-Redman, W.G. Tatton, Reduced mitochondrial membrane potential and altered responsiveness of a mitochondrial membrane megachannel in p53-induced senescence, Biochem. Biophys. Res. Commun. 261 (1) (1999) 123–130.
[62] B.R. Stab, L. Martinez, A. Grismaldo, A. Lerma, M.L. Gutiérrez, L.A. Barrera, et al., Mitochondrial functional changes characterization in young and senescent human adipose derived MSCs, Front. Aging Neurosci. 8 (DEC) (2016) 1–10.
[63] D. Wang, Y. Liu, R. Zhang, F. Zhang, W. Sui, L. Chen, et al., Apoptotic transition of senescent cells accompanied with mitochondrial hyper-function, Oncotarget 7 (19) (2016).
[64] M. Collado, J. Gil, A. Efeyan, C. Guerra, A.J. Schuhmacher, et al., Tumour biology: senescence in premalignant tumours, Nature 436 (7052) (2005) 642.
[65] D.J. Baker, T. Wijshake, T. Tchkonia, N.K. LeBrasseur, B.G. Childs, B. van de Sluis, et al., Clearance of p16Ink4a-positive senescent cells delays ageing-associated disorders, Nature 479 (7372) (2011) 232–236.
[66] M. Jaskelioff, F.L. Muller, J.H. Paik, E. Thomas, S. Jiang, A.C. Adams, et al., Telomerase reactivation reverses tissue degeneration in aged telomerase-defficient mice, Nature 469 (7328) (2011) 102–106.
[67] M. Lehmann, M. Korfei, K. Mutze, et al., Senolytic drugs target alveolar epithelial cell function and attenuate experimental lung fibrosis ex vivo, Eur. Respir. J. 50 (2) (2017).
[68] M.J. Schafer, T.A. White, et al., Cellular senescence mediates fibrotic pulmonary disease, Nat. Commun. 8 (2017) 14532.
[69] a L. Hecker, N.J. Logsdon, et al., Reversal of persistent fibrosis in aging by targeting Nox4-Nrf2 redox imbalance, Sci. Transl. Med. 6 (2014) 231ra47;
b Y.Y. Sanders, H. Liu, G. Liu, et al., Epigenetic mechanisms regulate NADPH oxidase-4 expression in cellular senescence, Free Radic. Biol. Med. 79 (2015) 197–205.
[70] A. Soto-Gamez, M. Demaria, Therapeutic interventions for aging: the case of cellular senescence, Drug Discov. Today 22 (5) (2017) 786–795.
[71] C.E. Burd, J.A. Sorrentino, K.S. Clark, D.B. Darr, J. Krishnamurthy, et al., Monitoring tumorigenesis and senescence in vivo with a p16(INK4a)-luciferase model, Cell. 152 (1–2) (2013) 340–351.
[72] C. Correia-Melo, J.F. Passos, Mitochondria: are they causal players in cellular senescence? Biochim. Biophys. Acta 1847 (11) (2015) 1373–1379.
[73] M.E. Lleonart, A. Arter-Castro, H. Kondoh, Senescence induction; a possible cacer therapy, Mol. Cancer. 8 (3) (2009).
[74] E. González-Gualda, M. Páez-Ribes, B. Lozano-Torres, Galacto-conjugation of navitoclax as an efficient strategy to increaase senolytic specificity and reduce platelet toxicity. Aging Cell (2020) e13142.